



Published in final edited form as:

IEEE Trans Plasma Sci IEEE Nucl Plasma Sci Soc. 2006 June ; 34(3): 518–523.

Operational Characteristics of a 14-W 140-GHz Gyrotron for Dynamic Nuclear Polarization

Colin D. Joye

Student Member, IEEE, The Plasma Science and Fusion Center, Massachusetts Institute of Technology, Cambridge, MA 02139 USA (e-mail: cjoye@mit.edu).

Robert G. Griffin

Member, IEEE, The Department of Chemistry and the Francis Bitter Magnet Laboratory, Massachusetts Institute of Technology, Cambridge, MA 02139 USA.

Melissa K. Hornstein

Member, IEEE, The Naval Research Laboratory, Washington, DC 20375 USA.

Kan-Nian Hu

Member, IEEE, The Department of Chemistry and the Francis Bitter Magnet Laboratory, Massachusetts Institute of Technology, Cambridge, MA 02139 USA.

Kenneth E. Kreischer

Member, IEEE, The Northrop Grumman Corporation, Electronics Systems, Rolling Meadows, IL 60008 USA.

Melanie Rosay

Member, IEEE, The Bruker BioSpin Corporation, Billerica, MA 01821 USA.

Michael A. Shapiro

Member, IEEE, The Plasma Science and Fusion Center, Massachusetts Institute of Technology, Cambridge, MA 02139 USA (e-mail: cjoye@mit.edu).

Jagadishwar R. Sirigiri

Member, IEEE, The Plasma Science and Fusion Center, Massachusetts Institute of Technology, Cambridge, MA 02139 USA (e-mail: cjoye@mit.edu).

Richard J. Temkin

Fellow, IEEE, The Plasma Science and Fusion Center, Massachusetts Institute of Technology, Cambridge, MA 02139 USA (e-mail: cjoye@mit.edu).

Paul P. Woskov

Senior Member, IEEE, The Plasma Science and Fusion Center, Massachusetts Institute of Technology, Cambridge, MA 02139 USA (e-mail: cjoye@mit.edu).

Abstract

The operating characteristics of a 140-GHz 14-W long pulse gyrotron are presented. The device is being used in dynamic nuclear polarization enhanced nuclear magnetic resonance (DNP/NMR) spectroscopy experiments. The gyrotron yields 14 W peak power at 139.65 GHz from the TE(0,3) operating mode using a 12.3-kV 25-mA electron beam. Additionally, up to 12 W peak has been observed in the TE(2,3) mode at 136.90 GHz. A series of mode converters transform the TE(0,3) operating mode to the TE(1,1) mode. Experimental results are compared with nonlinear simulations and show reasonable agreement. The millimeter-wave output beam was imaged in a single shot using

a pyroelectric camera. The mode patterns matched reasonably well to theory for both the TE(0,1) mode and the TE(1,1) mode. Repeatable mode patterns were obtained at intervals ranging from 0.8 s apart to 11 min apart at the output of the final mode converter.

Keywords

Dynamic nuclear polarization; gyrotron; millimeter wave

I. Introduction

A 140-GHz 14-W-long pulse gyrotron is in use for dynamic nuclear polarization (DNP) enhanced nuclear magnetic resonance (NMR) spectroscopy experiments in the Francis Bitter Magnet Laboratory at the Massachusetts Institute of Technology (MIT), Cambridge. In order to increase the signal-to-noise ratio (SNR) of the spectrum, the sample is polarized by millimeter-wave radiation (MMW) introduced into the DNP probe near the electron Larmor frequency and by radio frequency radiation near the nuclear Larmor frequencies. SNR enhancement factors on the order of several hundred are possible using this technique [1], [2]. A number of modest power, high-frequency gyrotrons have been built for various DNP applications recently [3]-[5].

A gyrotron is a vacuum electron device (VED) employing a strong magnetic field, an electron beam, and an electromagnetically resonant cavity. Detailed descriptions of the physics and engineering features of the gyrotron may be found in several recent books [6]-[8]. The electrons gyrate around the magnetic field lines at the electron cyclotron frequency in a helical motion as they traverse through the tube structure. Inside the resonator, a fast wave interaction between the electron beam and MMW takes place which converts some of the transverse kinetic energy of the electron beam into MMW energy in the form of TE_{mn} electromagnetic modes. The transverse dimensions of the resonator can be of the order of several wavelengths. This enables the generation of high average power at high frequencies in gyrotrons due to lower thermal losses in the resonator walls when compared to conventional slow wave devices, such as traveling wave tubes and backward wave oscillators.

This gyrotron is based on an older design that was developed and used for plasma diagnostics [9]. That gyrotron was modified and used successfully for DNP/NMR research, and is described in detail in [10]. The gyrotron used a high-voltage electron gun, which operated at 40 to 65 kV, requiring cumbersome oil cooling. The gun was also a triode configuration with a cathode, modulation anode, and a ground anode. The present 140-GHz gyrotron system contains a new diode electron gun, which operates at a low voltage of 12.3 kV at up to 25 mA. Output pulses up to 15 s long at 50% duty cycle are possible. For single-pulse operation, an emission period as long as 5 min is easy to achieve. The lower voltage has resulted in a much simpler power supply system.

This paper reports the operating characteristics of the present 140-GHz 14-W gyrotron. The presentation of this material is organized as follows: First, a brief overview of the gyrotron is presented, followed by the results of the experiments performed to map the operating characteristics which include a mode map, power and frequency measurements, simulations, and pyroelectric camera images of the mode patterns. In the final section, concluding remarks are given.

II. Overview

The system block diagram is shown in Fig. 1. The hollow, annular electron beam is emitted from a thin, indirectly heated ring cathode of a magnetron injection gun (MIG) at one extreme

of the tube. This beam is guided and compressed through the cavity circuit by a solenoidal magnetic field with a peak value of approximately 5.08 T centered in the interaction region. The potential between the cathode and anode surfaces of the MIG is -12.3 kV and the current can be controlled from about 10 to 30 mA by adjusting the alternating current (ac) heater filament current. The magnetic field at the cathode is fine tuned by means of a water cooled copper coil bolted to the outside of the superconducting magnet Dewar, which is capable of altering the cathode field by about ± 0.2 T. The vacuum base pressure is on the 10^{-9} torr scale and the operating pressure is kept well below 10^{-7} torr. A summary of the operating parameters for this gyrotron is presented in Table I.

The present gyrotron tube differs from the original tube mostly in the region of the electron gun. Most of the parts of the present electron gun were built by MIT and assembled by MIT, with exception of the cathode stalk, which was built by Semicon Associates¹ (Lexington, KY). The previous design of the tube had very inefficient pumping with a small constriction, three 90° bends and nearly a meter of vacuum lines from the emitter region to a 40 L/s vacuum pump. In addition, the pumping configuration prevented proper baking of the entire gyrotron tube under vacuum. The present gun was designed to allow for direct pumping of the electron gun via four slots (0.74×4.22 cm) cut through the cathode stalk for efficient pumping of the emitter (Fig. 2). The cathode stalk alignment is controlled by shims between the two flanges at the base of the gun. The shims limit the depth of the flange cut into the copper gasket. The ac heater is insulated from the high voltage with a ceramic feed-through while two large ceramic breaks insulate the anode and the 8 L/s vacuum ion pump. The electron gun vacuum pump is located about 23 cm in a straight line from the emitter. The present design also allows for possible removal of the gyrotron tube from the superconducting magnet without disassembly (except for removal of the ion pump magnets). The tube can withstand being baked out at up to 200° C

The electron gun was designed with a beam pitch factor of approximately 1.6, a beam radius of 1.86 mm (corresponding to the second radial maximum of the TE_{03} mode), and transverse optical velocity spread of 3.2% from simulations at the operating point using EGUN [11]. The calculated total transverse velocity spread including surface roughness and thermal effects [12] is approximately 6%. The actual beam pitch factor during operation is very sensitive to the magnetic field at the cathode.

After the electron beam passes through the beam tunnel, it enters the resonator section of the cavity (Fig. 3). On the end of the cavity through which the electron beam enters, the resonator radius is downtapered toward the electron gun at an angle of 1° such that it is cut off to the operating MMW fields in the resonator in order to prevent power from leaking out. The gyrotron cavity resonator is a circular waveguide straight section 28.25 mm long (approximately 13 wavelengths) with a radius of 3.48 mm. In this section, the cyclotron resonance maser (CRM) instability causes some of the perpendicular momentum in the electron beam to be converted into MMW energy near the cyclotron frequency of the electrons. At the end of the straight section, the cavity radius is uptapered with a 2° angle. The uptaper allows this MMW radiation to diffract out of the cavity and is designed to prevent further interaction of the MMW and electron beam. The theoretical diffractive Q of the cavity is almost 7000. The theoretical ohmic Q is approximately 28 000, but we estimate a much smaller value of about 14 000. The calculated temperature rise in the cavity during CW operation is approximately 0.2 K.

¹<http://www.semiconassociates.com>

The cavity is water cooled to prevent it from becoming de-tuned due to thermal expansion. The heat lost by the finite electrical conductivity of the copper is carried away by a water-cooled jacket brazed to the cavity.

After the spent electron beam exits the cavity circuit, it is collected at the other extreme of the tube by a water-cooled collector.

The MMW radiation travels through the uptaper and collector sections and then propagates through a TE_{03} to TE_{02} axisymmetric rippled wall mode converter of $N = 5$ beat periods followed by a TE_{02} to TE_{01} mode converter that also uses $N = 5$ periods [9]. The efficiencies of each of these mode converters has been measured to over 99% [10]. A mirror and miter joint at the end of the second mode converter prevent stray electrons from striking the vacuum window and carry the TE_{01} mode out of the gyrotron via a 1.27-cm-diameter overmoded copper waveguide. The fused quartz window is 2.73 cm in diameter and 3.43 mm thick and is designed to be transparent to MMW at 140 GHz. An all-metal valve was added close to the quartz window for connecting a turbo pump during bake-out.

Outside of the gyrotron, the TE_{01} mode is converted to the TE_{11} mode using a serpentine rippled wall mode converter [13]. This mode converter was designed using coupled mode equations for a circular waveguide bent in a circular arc where one beat period is made up of two bent 6.53 cm long, 1.27 cm diameter copper sections with a bending radius of 1.21 m placed end to end. The structure consists of seven such period yielding a design efficiency of over 94% at 140 GHz [14]. The structure was created by heating a copper pipe packed with sand and forcing it into a carved aluminum block to create the serpentine shape.

After this mode converter, the TE_{11} power is finally sent to the DNP probe by means of an over moded cylindrical 1.27-cm-diameter copper waveguide. The losses in this waveguide total approximately 7 dB and the bulk of these losses appear in a downtaper section just before entry to the DNP probe [10], [15], [16].

III. Experimental Results

A harmonic heterodyne receiver system was used to measure the frequency of the gyrotron output. The receiver employs a low frequency local oscillator (LO) of between 8–18 GHz and a harmonic mixer to mix the gyrotron signal with a harmonic of the LO (typically the tenth harmonic). The intermediate frequency (IF) is limited to 150–500 MHz by bandpass filters and is amplified by a series of solid state amplifiers. The result is fast fourier analyzed on an oscilloscope. The LO frequency is counted by a frequency counter, multiplied by the harmonic number, and added to or subtracted from the IF to determine the gyrotron frequency. The system can accurately measure the gyrotron frequency to within 1 MHz or better.

The output power was measured using a 4-in analog Peltier junction dry calorimeter from Scientech Inc. We modified this calorimeter by applying a thin (approximately 0.3 mm) absorbing layer of 3M Nextel paint to enhance the absorption of MMW [17]. The power absorption has recently been measured at 140 GHz to be 82% using an E8363B Agilent Precision Network Analyzer (PNA) with Olsen Microwave Lab millimeter wave extenders that work in the WR-8 (90–140 GHz) band.

A. Mode Map

The mode map for this gyrotron was generated by holding the operating voltage fixed at 12.3 kV while scanning the main magnetic field and the gun coil magnetic field (Fig. 4). The filament current was adjusted to keep the beam current at a nominal value of around 25 mA. The gyrotron was set to a duty cycle of 50% and a pulse length of 1 s.

Table II lists the different modes and frequencies observed in generating this mode map. The measured frequencies were matched to theory through a cold cavity code originally developed by Fliflet and Read [18]. In this cold cavity code, the radius of the resonator had to be decreased from its theoretical value of 3.480 to 3.478 mm to match the measured frequency of the TE_{031} operating mode. The change in radius is consistent with the manufacturing tolerance of the cavity. The other frequencies were then consistent with the measured data. The axial profiles resulting from the cold cavity code indicated the axial mode index, while the resonant frequency and diffractive Q are output values from the code.

A transient frequency shift of approximately 0.2 MHz during the first 3 s of the pulse at 12.3 kV has been observed due to the thermal expansion of the cavity. The sensitivity of frequency shift due to thermal expansion was found to be -2.2 MHz/K. Additionally, there are frequency fluctuations due to the power supply regulation on the order of 0.2 MHz. The gyrotron's frequency fluctuation sensitivity due to voltage ripple has been determined to be 0.14 ppm/V [10], [19].

The interaction was modeled using a nonlinear time dependent simulation code MAGY, developed jointly at the University of Maryland and the Naval Research Laboratory [20]. The MAGY simulation is compared to the measured power from this cavity design in the TE_{031} mode in Fig. 5 over a range of main magnetic field. Using a calculated transverse velocity spread of 6% for the simulation and a conductivity of half that of ideal copper for the cavity walls, a beam pitch factor of 1.45 resulted in a good fit to the measured data. Other operating parameters were the same as in Table I. The actual value of beam pitch factor in experiment is very sensitive to the magnetic field at the cathode, and it appears that the low beam pitch factor, lower than the design value of 1.6, is limiting the output power.

The theoretical minimum oscillation start current for the TE_{031} operating mode was calculated to be 10 mA [21] at 12.3 kV, 5.08 T, and a total Q factor of approximately 5000. This simulated value matched the experimentally observed value under the same conditions.

B. Millimeter-Wave Imaging

The MMW output of the gyrotron was imaged using the Pyrocam III pyroelectric camera detector from Spiricon, Inc. [22]. This camera consists of an array of 124-by-124 calibrated $LiTaO_3$ pyroelectric sensors with a spacing of 100 μm between each pixel. There is a motorized chopper blade over the sensor array which can operate at 48 or 24 Hz, or can be externally triggered for pulse operation. The chopper is necessary for CW beams because the pyroelectric crystals are only sensitive to changes in signal. Although this camera was designed for laser applications for wavelengths in the Terahertz range and was tested at frequencies as low as 0.2 THz (1.5 mm wavelength) [23], we have found that it also works very well at microwave frequencies where the wavelength is above 2 mm, provided the waveguide aperture is small enough and the maximum power rating for the sensor is not exceeded. To our knowledge, this is the first time that a millimeter wave beam of such long wavelength has been directly imaged with a high resolution and high speed camera. Similar measurements have also been made of a 250 GHz (1.2-mm wavelength) gyrotron beam at MIT by Bajaj *et al.* [24].

The pyroelectric camera provides the operator the advantage of viewing the mode pattern in real time and can thus be used to follow the beam shape over time in increments as small as tens of milliseconds. This may be advantageous for systems where the power output is not stable over time. It can also be set up at various points in a beam system as an aid in alignment and measurement. The pyroelectric camera ratings are listed in Table III.

Two measurements were made using the camera: one at the gyrotron output window and the other at the end of the TE_{01} to TE_{11} mode converter. In both cases, the pyroelectric camera

was placed as close to the output as the chopper would allow, with the sensor less than three wavelengths away from the output aperture in both cases.

The measured and calculated mode patterns are shown in Fig. 6(a) and (b), respectively, near the quartz window where the pattern should match the TE_{01} mode, and in Fig. 6(c) and (d) after the final mode converter where the pattern should match the TE_{11} mode. The experimental patterns were captured at low power (approximately 0.4 W average) to avoid damage to the pyroelectric camera. While there is evidence of mode mixtures, the measured mode patterns matched well enough to the theoretical patterns for our present application.

Fig. 7(a) and (b) shows two adjacent images of the final mode converter output captured 0.8 s apart. Fig. 7(c) and (d) shows the same mode captured 11 min apart. These images show the excellent repeatability of the gyrotron pulses and the capability of the camera to monitor the long term stability of the gyrotron output beam.

IV. Conclusion

A 140-GHz 14-W long pulse DNP gyrotron has been operationally characterized. A mode map of the operating regimes of the device has been generated and shows 14 W peak power from a 12.3-kV, 25-mA electron beam with a radius of approximately 1.86 mm and an estimated perpendicular momentum spread of 6% for the TE_{03} operating mode at 139.65 GHz. The design value of the beam pitch factor was approximately 1.6, but we have found that a value of 1.45 in simulation fits the measured data well. Additionally, up to 12 W peak power has been observed in the TE_{23} mode at 136.90 GHz. The measured start current values agree well with theory. The nonlinear code MAGY has been used to analyze the output power with good agreement assuming a lower value of beam pitch factor in the electron beam.

For the first time on the 140-GHz gyrotron system, a pyroelectric camera has been used to image the entire mode pattern in a single capture. Repeatable images were captured over a wide range of time scales. The measured mode patterns for the 140-GHz gyrotron matched reasonably well for both the TE_{01} mode and the TE_{11} mode. The pyroelectric camera is a promising technology that offers wide dynamic range, high sensitivity and real time image capture at up to several frames per second. These features make it useful for such tasks as aligning waveguide and quasi-optical systems, and for long term monitoring of the output beam.

Acknowledgment

The authors would like to thank J. Bryant for his assistance with the gyrotron measurements.

Biographies

Colin D. Joye (S'03) received the B.S. degree in electrical engineering and computer science from Villanova University, Villanova, PA, in 2002, and the M.S. degree in electrical engineering and computer science, in 2004, from Massachusetts Institute of Technology (MIT), Cambridge, where he is currently working toward the Ph.D. degree.

In 2002, he joined the Waves and Beams Division at the Plasma Science and Fusion Center (PSFC), MIT as a Research Assistant. His current research interests include gyrotron oscillator and amplifier sources at the millimeter and submillimeter wavelengths.



Robert G. Griffin received the B.S. degree in chemistry from the University of Arkansas, Fayetteville, in 1964 and the Ph.D. degree in physical chemistry from Washington University, St. Louis, MO, in 1969. He did his postdoctoral research in physical chemistry at the Massachusetts Institute of Technology (MIT), Cambridge, with Prof. J. S. Waugh.

In 1972, after completing his postdoctoral training, he assumed a staff position at the Francis Bitter National Magnet Laboratory (FBML), MIT. In 1984, he was promoted to Senior Research Scientist, and was appointed to the faculty in the Department of Chemistry, MIT, in 1989. In 1992, he became Director of the FBML and is concurrently Director of the MIT-Harvard Center for Magnetic Resonance, where he had been Associate Director since 1989. He has published more than 300 articles concerned with magnetic resonance methodology and applications of magnetic resonance (NMR and EPR) to studies of the structure and function of a variety of chemical, physical and biological systems. In the last decade, this research has focused on the development of methods to perform structural studies of membrane and amyloid proteins and on the utilization of high-frequency (>100 GHz) microwaves in EPR experiments and in the development of DNP/NMR experiments at these frequencies. He has served on numerous advisory and review panels for the National Science Foundation and the National Institutes of Health.



Melissa K. Hornstein (S'97–M'05) received the B.S. degree in electrical and computer engineering from Rutgers University, New Brunswick, NJ, in 1999, and the M.S. and Ph.D. degrees in electrical engineering and computer science from the Massachusetts Institute of Technology (MIT), Cambridge, MA, in 2001 and 2005, respectively.

From 2000 to 2005, she was a Research Assistant at the Plasma Science and Fusion Center and the Francis Bitter Magnet Laboratory, MIT. She was involved in the design, development, testing, and analysis of a novel submillimeter wave second harmonic gyrotron oscillator, as well as other projects in the millimeter and submillimeter regime. Since 2005, she has been at the Naval Research Laboratory as an NRC postdoc in the Plasma Physics Division. Her research interests include terahertz sources and their applications, such as enhanced nuclear magnetic resonance spectroscopy via dynamic nuclear polarization.

Kan-Nian Hu received the B.A. and M.S. degrees in chemistry from National Taiwan University, Taipei, Taiwan, in 1996 and 1998, respectively. He is currently working toward the Ph.D. degree in physical chemistry at the Massachusetts Institute of Technology (MIT), Cambridge.

Since 2000, he has been a Research Assistant with the Francis Bitter Magnet Laboratory, MIT, where his research involves the development of DNP for sensitivity enhancement in NMR spectroscopy, in particular designing polarizing agents for DNP at high magnetic fields above 5 Tesla.



Kenneth E. Kreischer (M'88) received the B.S. degree in physics and the Ph.D. degree in nuclear engineering from the Massachusetts Institute of Technology, Cambridge, in 1976 and 1981, respectively.

He remained at MIT from 1981 to 2000, where he was a Principal Research Scientist at the Plasma Science and Fusion Center, MIT. His main responsibility at MIT was overseeing the experimental research activities of the Waves and Beam Division. A major area of research was the design and testing of MW gyrotron oscillators operating at 100–300 GHz suitable for the heating of fusion plasmas. Other responsibilities included the development of a high gradient accelerator operating at 17 GHz, an RF photocathode gun capable of producing a high brightness electron beam, and submillimeter instrumentation that increases the sensitivity of EPR and NMR spectrometers used in chemistry molecular research. He joined Northrop Grumman Corporation in 2000, and is presently Director of the Vacuum Electronics Technology Research and Development Group. This group is responsible for developing high-power, broadband microwave power modules that are used in ECM transmitters. They are also designing and testing novel THz technology that will be used as part of a high resolution imaging system being developed by DARPA. In addition to THz instrumentation and broadband sources, his research interests also include high frequency sources suitable for radar and communication, nonlethal active denial systems based on high-power microwaves, field emission electron sources, and agile beam steering.

Dr. Kreischer is presently a member of the American Physical Society and Phi Beta Kappa.

Melanie Rosay photograph and biography not available at the time of publication.

Michael A. Shapiro (M'01) received the Ph.D. degree in radio physics from the University of Gorky, Gorky, Russia, in 1990.

In 1995, he joined the Plasma Science and Fusion Center, Massachusetts Institute of Technology (MIT), Cambridge, where he is currently Head of the Gyrotron Research Group. His research interests include vacuum microwave electron devices, high power gyrotrons, dynamic nuclear polarization spectroscopy, high gradient linear accelerator structures, quasi-optical millimeter-wave components, and photonic bandgap structures.



Jagadishwar R. Sirigiri (S'98–M'02) received the B.Tech. degree in electronics and communication engineering from the Institute of Technology, Banaras Hindu University (BHU), India, in 1996, and the M.S. and Ph.D. degrees in electrical engineering and computer science from the Massachusetts Institute of Technology (MIT), Cambridge, in 1999 and 2002, respectively.

From 1994 to 1996, he was associated with the Center of Research in Microwave Tubes, BHU, where his research areas included TWTs and gyro-TWTs. From 1996 to 1998, he was with Global Research and Development, Wipro Infotech, Ltd., where he worked in the multimedia research group. Since 2002, he has been a Postdoctoral Research Associate at the Plasma Science and Fusion Center, MIT. He is involved in the design and development of novel high-power gyrotrons and gyrotron amplifiers at millimeter-wave frequencies. His research interests include novel microwave sources and amplifiers in the millimeter and submillimeter regime such as the gyrotron, quasi-optical structures, and photonic band gap (PBG) structures and their applications in microwave vacuum electronics.



Richard J. Temkin (M'87–F'94) received the B.A. degree in physics from Harvard College, Cambridge, MA, and the Ph.D. degree in physics from the Massachusetts Institute of Technology (MIT), Cambridge.

From 1971 to 1974, he was a Postdoctoral Research Fellow in the Division of Engineering and Applied Physics, Harvard University. Since 1974, he has been with MIT, first at the Francis Bitter National Magnet Laboratory and later at the Plasma Science and Fusion Center (PSFC) and the Department of Physics. He currently serves as a Senior Scientist in the Physics Department, as Associate Director of the PSFC, and Head of the Waves and Beams Division, PSFC. His research interests include novel vacuum electron devices such as the gyrotron and free electron laser, advanced, high-gradient electron accelerators, quasi-optical waveguides and antennas at millimeter wavelengths, plasma heating, and electron spin resonance spectroscopy. He has been the author or coauthor of over 200 published journal articles and book chapters and has been the editor of six books and conference proceedings.

Dr. Temkin is a Fellow of the American Physical Society and The Institute of Physics, London, U.K. He has been the recipient of the Kenneth J. Button Prize and Medal of The Institute of Physics, London and the Robert L. Woods Award of the Department of Defense for Excellence in Vacuum Electronics research.



Paul P. Woskov (S'74–M'76–SM'99) received the Ph.D. degree in electrical engineering from the Rensselaer Polytechnic Institute, Troy, NY, in 1976.

In 1976, he joined the Francis Bitter National Magnet Laboratory, Massachusetts Institute of Technology (MIT), Cambridge, where, since 1980 he has been with the MIT Plasma Science and Fusion Center. He is currently a Principal Research Engineer and Associate Division Head of the Plasma Technology Division. His principal interests include plasma diagnostics, fusion energy, millimeter-wave technologies, and environmental applications of plasmas and millimeter waves.

Dr. Woskov is a member of the American Physical Society, the American Chemical Society, and the American Association for the Advancement of Science.



References

1. Wind RA, et al. Applications of dynamic nuclear polarization in ^{13}C NMR in solids. *Progress NMR Spectroscopy* 1985;17:33–67.
2. Becerra LR, Gerfin GJ, Temkin RJ, Singel DJ, Griffin RG. Dynamic nuclear polarization with a cyclotron resonance maser at 5 Tesla. *Phys. Rev. Lett* 1993;117:3561–3564. [PubMed: 10055008]
3. Kreisler, KE.; Farrar, C.; Griffin, R.; Temkin, R. The use of a 250 GHz gyrotron in a DNP/NMR spectrometer; *Proc. 23rd Int. Conf. Infrared Millim. Waves*; 1998. p. 341-357.
4. Idehara T, Ogawa I, Mitsudo S, Pereyaslavets M, Nishida N, Yoshida K. Development of a frequency tunable, medium power gyrotron (gyrotron FU series) as submillimeter wave radiation sources. *IEEE Trans. Plasma Sci* Apr.;1999 27(2):340–354.
5. Hornstein MK, Bajaj VS, Griffin RG, Kreisler KE, Mastovsky I, Shapiro MA, Sirigiri JR, Temkin RJ. Second harmonic operation at 460 GHz and broadband continuous frequency tuning of a gyrotron oscillator. *IEEE Trans. Electron Devices* May;2005 52(5):798–807.
6. Barker, RJ.; Luhmann, NC.; Booske, JH.; Nusinovich, GS. *Modern Microwave and Millimeter-Wave Power Electronics*. Wiley-IEEE; Hoboken, NJ: 2005.
7. Nusinovich, GS. *Introduction to the Physics of Gyrotrons*. Johns Hopkins Univ. Press; Baltimore, MD: 2004.
8. Kartikeyan, MV.; Borie, E.; Thumm, MKA. *Gyrotrons*. Springer-Verlag; New York: 2004.
9. Machuzak JS, Woskoboinikow P, Mulligan WJ, Cohn DR, Gerver M, Guss W, Mauel M, Post RS, Temkin RJ. 137-GHz gyrotron diagnostic for instability studies in Tara. *Rev. Sci. Instrum* 1986;57(8):1983–1985.
10. Becerra LR, Gerfin GJ, Bellew BF, Bryant JA, Hall DA, Inati SJ, Weber RT, Un S, Prisner TF, McDermott AE, Fishbein KW, Kreisler KE, Temkin RJ, Singel DJ, Griffin RG. A spectrometer for dynamic nuclear polarization and electron paramagnetic resonance at high frequencies. *J. Mag. Reson* 1995;117:28–40.
11. Hermannsfeldt WB. EGUN—An electron optics and gun design program Stanford Linear Accelerator Center. Oct.;1988 Tech. Rep. SLAC-331, UC-28
12. Baird JM, Lawson W. Magnetron injection gun (MIG) design for gyrotron applications. *Int. J. Electron* 1986;61(6):953–967.
13. Moeller C. Mode converters used in the Doublet III ECH microwave system. *Int. J. Electron* 1982;53:587–593.
14. Hornstein, M. Design of a 460 GHz second harmonic gyrotron oscillator for use in dynamic nuclear polarization. Dept. Elec. Eng. Comp. Sci., Massachusetts Institute of Technology; Cambridge: 2001. M.S. thesis
15. Rosay, M. Sensitivity enhanced nuclear magnetic resonance in biological solids. Dept. Chem., Massachusetts Institute of Technology; Cambridge: 2001. Ph.D. dissertation
16. Hornstein, M. A continuous wave second harmonic gyrotron oscillator at 460 GHz. Dept. Elec. Eng. Comp. Sci., Massachusetts Institute of Technology; Cambridge: 2005. Ph.D. dissertation
17. Kreisler KE, Schutkeker JB, Danly BG, Mulligan WJ, Temkin RJ. High efficiency operation of a 140 GHz pulsed gyrotron. *Int. J. Electron* 1984;57(6):835–850.
18. Fliflet AW, Read ME. Use of weakly irregular waveguide theory to calculate eigenfrequencies, Q values and RF field functions for gyrotron oscillators. *I. J. Electron* 1981;51:475–484.

19. Hall, DA. Dynamic nuclear polarization of biological systems at high magnetic fields. Massachusetts Institute of Technology; Cambridge: 1998. Ph.D. dissertation
20. Botton M, Antonsen TM Jr. MAGY: a time-dependent code for simulation of slow and fast microwave sources. *IEEE Trans. Plasma Sci Jun.*;1998 26(3):882–892.
21. Danly BG, Temkin RJ. Generalized nonlinear harmonic gyrotron theory. *Phys. Fluids* 1985;29(2): 561–567.
22. Pyrocam III. Model PY-III-C-B Spiricon, Inc.; Logan, UT: 2001.
23. Pyrocam III. New Product Announcement Spiricon, Inc.; Logan, UT: Jan.. 2003
24. Bajaj VS, et al. A Long-Term, Stable, CW 250 {GHz} Gyrotron. unpublished



Fig. 1. Gyrotron block diagram showing the electron gun (MIG), main magnet, cavity, collector, internal mode converters, and quartz window.



Fig. 2.
Diagram of the current electron gun showing the location of the pumping slots and vacuum pump.

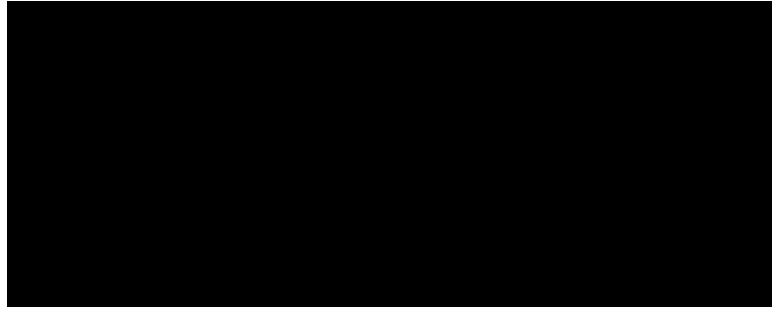


Fig. 3. Schematic of the resonator showing (a) the downtaper, (b) cavity straight section, and (c) uptaper section along with (d) the simulated electric field profile of the TE_{031} mode in arbitrary units.

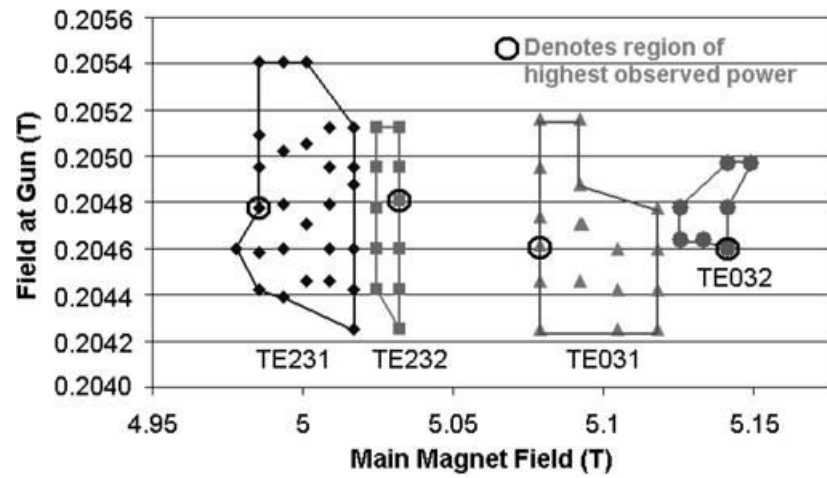


Fig. 4. Mode map for the 140-GHz gyrotron. Heavy circles indicate the location of highest observed power in each mode.

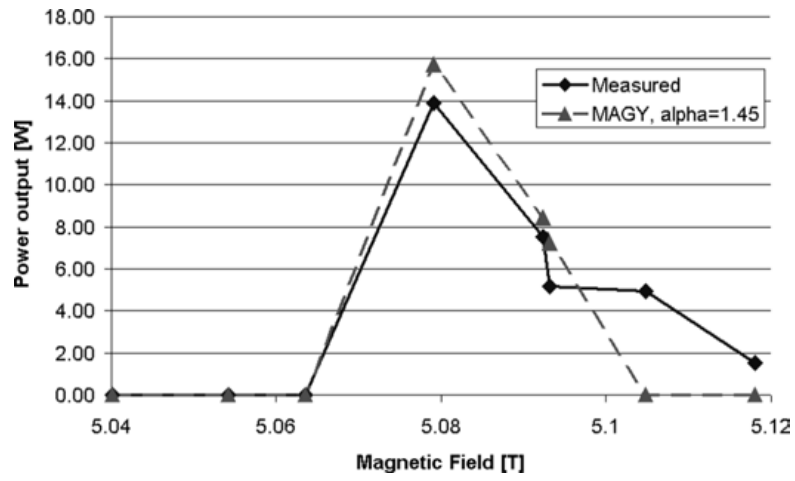


Fig. 5. Power output for the TE_{031} mode versus main magnetic field comparing the measurement to simulation.

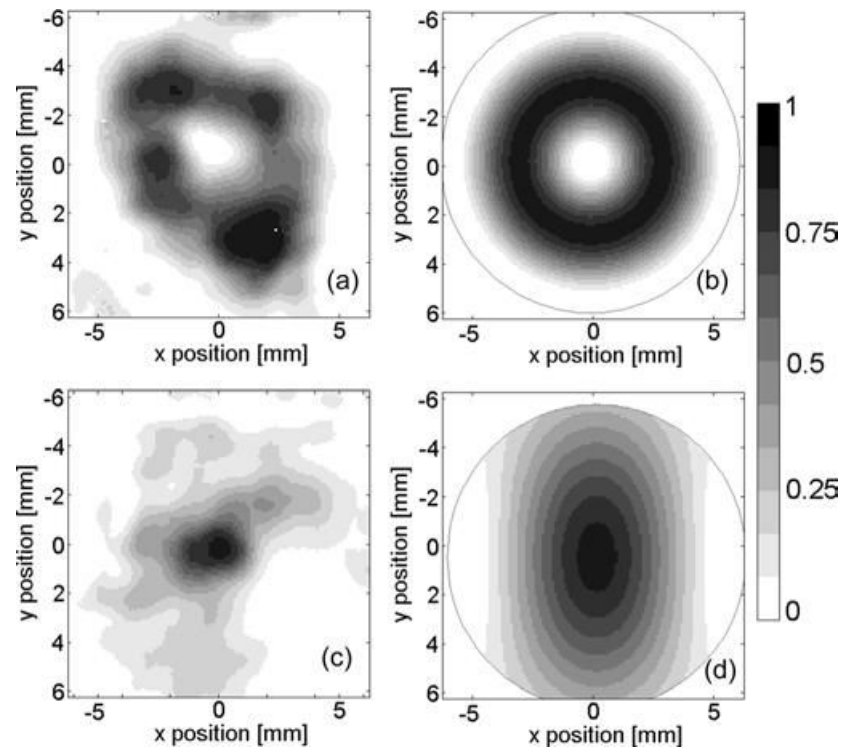


Fig. 6. (a) Measured gyrotron output. (b) Theoretical TE₀₁ mode. (c) Measured final mode converter output. (d) Theoretical TE₁₁ mode. Scale is normalized linear power.

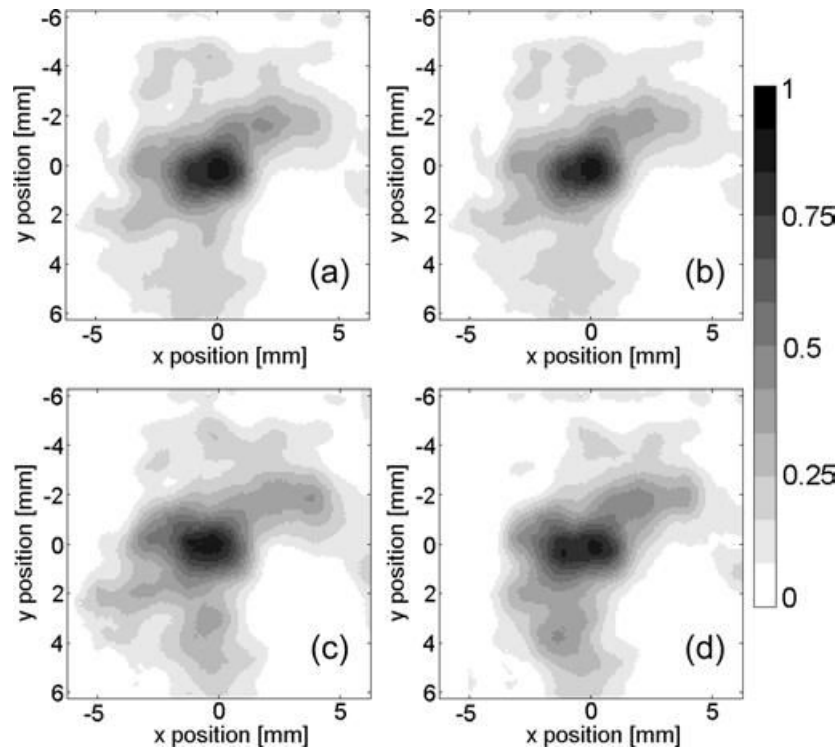


Fig. 7. Mode measurements at the output of the final mode converter (a)–(b) 0.8 s apart and (c)–(d) 11 min apart. Scale is normalized linear power.

TABLE I

Operating Parameters

| | |
|--------------------------|------------------|
| Operation Voltage, V_0 | 12.3 kV |
| Beam Current, I_0 | 0.025 A |
| Operating Mode | TE ₀₃ |
| Tube Output Mode | TE ₀₁ |
| Magnetic Field, B_0 | 5.08 T |
| Output Power | 14 W |
| Efficiency | 4% |
| Duty factor | 50% |

TABLE II

| Mode Table | | | | |
|------------|-------------------------------|--|-----------|-----------------|
| Mode | Calc freq ^{<i>l</i>} | Calc Q _{diff} ^{<i>l</i>} | Meas freq | Peak meas pwr |
| TE031 | 139.65 | 6950 | 139.65 | 13.9W at 24.6mA |
| | | | 139.76 | 1.5 at 24.8 |
| TE032 | 139.88 | 1750 | 139.87 | 1.2 at 24 |
| | | | 139.91 | 8.0 at 25.6 |
| | | | 136.90 | 11.8 at 24.9 |
| TE231 | 136.86 | 6615 | 136.90 | 1.9 at 23.8 |
| | | | 137.13 | 8.2 at 24.0 |
| TE232 | 137.08 | 1660 | 137.13 | |

^{*l*}Calculated using Cold Cavity code, frequencies in GHz.

TABLE III

Pyroelectric Camera Ratings at 24 HZ [22]

| | |
|------------------------|--------------------------------|
| Maximum power | 2 W over whole array |
| Maximum power density | 8 W/cm ² |
| Minimum Signal Level | 2.2 mW/cm ² |
| Noise equivalent power | 45 nW/Hz ^{1/2} /pixel |